Introduction

Wide azimuth (WAZ) has been established as an indispensable seismic acquisition and processing methodology for exploration and development objectives. This is especially relevant in the Gulf of Mexico (GoM). In comparison to a narrow azimuth (NAZ) survey, WAZ provides better subsurface illumination and fold coverage. Tilted Transverse Isotropic (TTI) model building has become a standard approach for processing WAZ data in the GoM. Because TTI accounts for polar anisotropy caused by bedding and stratification, in general it improves image focusing in pre-stack depth imaging and provides flatter common image gathers (CIGs) for WAZ data.

Recently, a range of methods has been implemented to acquire data with even greater azimuthal information. Examples of this are orthogonal wide azimuth (OWAZ), (Baldock, 2011), rich azimuth (RAZ) surveys (Howard, 2007), and coil shooting (Moldoveanu and Kapoor, 2009). An OWAZ survey was acquired in order to obtain a geometry that approaches Full Azimuth (FAZ). The two WAZ surveys, co-located in space, were acquired with identical (or nearly identical) acquisition geometries. The additional azimuth and offset information from the orthogonal survey is valuable in helping to improve the accuracy of the velocity model.

While the new acquisition technologies bring rich azimuthal information that better illuminates the subsurface, they also pose a challenge for depth imaging to be able to take into account azimuthal anisotropy beyond transverse isotropic (TI). TI describes anisotropy caused by thin layering of sediments with a scale that is smaller than the predominant wavelength. The axis of symmetry is perpendicular to the layers and thus assumes that the velocities are the same in the transverse plane regardless of azimuth (Thomsen, 1986). Although TI takes into account velocity differences between layer planes as well as polar direction, this may not be sufficient to describe the subsurface in areas where fractures are embedded within stratigraphic layers. In this case CIGs with different azimuths cannot be flattened with a single TTI model. There is a need within the industry for a more general model that describes azimuthal anisotropy in addition to polar anisotropy. ORT model can flatten all the CIGs for different azimuths as a more complex but more realistic model because orthorhombic anisotropy describes seismic velocity varying with azimuthal direction as well as polar direction.

Method

The workflow for orthorhombic model building is presented in Figure 1. Firstly, TTI tomography is performed to update ε_i and δ_i for each azimuth, where i refers to the i^{th} azimuth. Because each azimuth is updated individually, the gather flatness is improved with azimuth-variant ε_i andδ_i. These models of ε_i and δ_i are combined to fit into orthorhombic models (Li, 2012). Although there is approximation here, it is a flow for building an initial orthorhombic model.

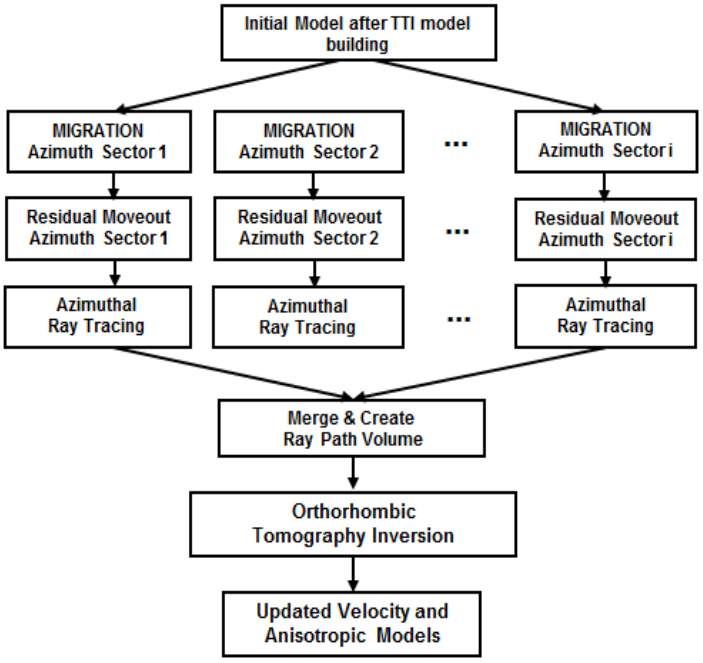

Figure 1 *The workflow for orthorhombic model building.*

OWAZ data was partitioned into six azimuth sectors. These azimuth sectors were of unequal size to maintain consistent fold between sectors. Curvature picking and ray-tracing were performed for each azimuth sector separately. The individual ray-trace volumes (ray-paths) were combined to create a

single ray-path volume which was then used to invert for a single orthorhombic model. The key for building orthorhombic models is to generate a set of $\varepsilon^{(1)}$, $\varepsilon^{(2)}$, $\delta^{(1)}$, $\delta^{(2)}$, $\delta^{(3)}$ (Tsvankin,1997) corresponding to the local fast velocity orientation α, which can solve the inconsistency of the moveout among azimuths. Coherence has been proved to be a useful tool for fault detection (Gersztenkorn and Marfurt, 1999). We use a hybrid similarity/dip measure to assist in the interpretation of faults and fractures and to get a geologically plausible fast velocity orientation, α.

Orthorhombic phase velocity equation is as follows, (Tsvankin, 1997),

$$V(\theta,\varphi) = V_0[1 + \delta(\varphi)sin^2\theta cos^2\theta + \epsilon(\varphi)sin^4\theta] \quad (1)$$

$$\delta(\varphi) = \delta^{(1)}sin^2\varphi + \delta^{(2)}cos^2\varphi \quad (2)$$

$$\varepsilon(\varphi) = \epsilon^{(1)}sin^4\varphi + \varepsilon^{(2)}cos^4\varphi + (2\varepsilon^{(2)} + \delta^{(3)})sin^2\varphi cos^2\varphi \quad (3)$$

It has the same form as the phase velocity in TI media, but with azimuth-dependent ε and δ. Here, θ is the polar angle and φ is the azimuthal angle. $\delta(\varphi)$ is an ellipse, while $\varepsilon(\varphi)$ is not an ellipse with $\delta^{(3)}$ contributing to ε.

Taking the derivative of Equation (1), the sensitivity of the travel time with respect to slowness and anisotropic parameters can be obtained. Figure 2 gives the plots of the derivatives for $\theta \in (0, 90)$ and $\varphi \in (0,360)$. $\frac{dt}{dS}$ is less than 1 because of anisotropic effects, while $\frac{dt}{dS} = 1$ for isotropic media. $\frac{dt}{d\delta^{(1)}}$ and $\frac{dt}{d\delta^{(2)}}$ have a perpendicular pattern, so do $\frac{dt}{d\varepsilon^{(1)}}$ and $\frac{dt}{d\varepsilon^{(2)}}$. Also, $\frac{dt}{d\delta^{(1)}}$ and $\frac{dt}{d\delta^{(2)}}$ have zero value at very near and far incident angles. Most non-zero values distribute in the middle angles, while $\frac{dt}{d\varepsilon^{(1)}}$ and $\frac{dt}{d\varepsilon^{(2)}}$ are zero at near angles and have big values at far incident angles. $\frac{dt}{d\delta^{(3)}}$ is zero inside both vertical symmetric planes and has non-zero values only at far angles outside the vertical symmetric planes.

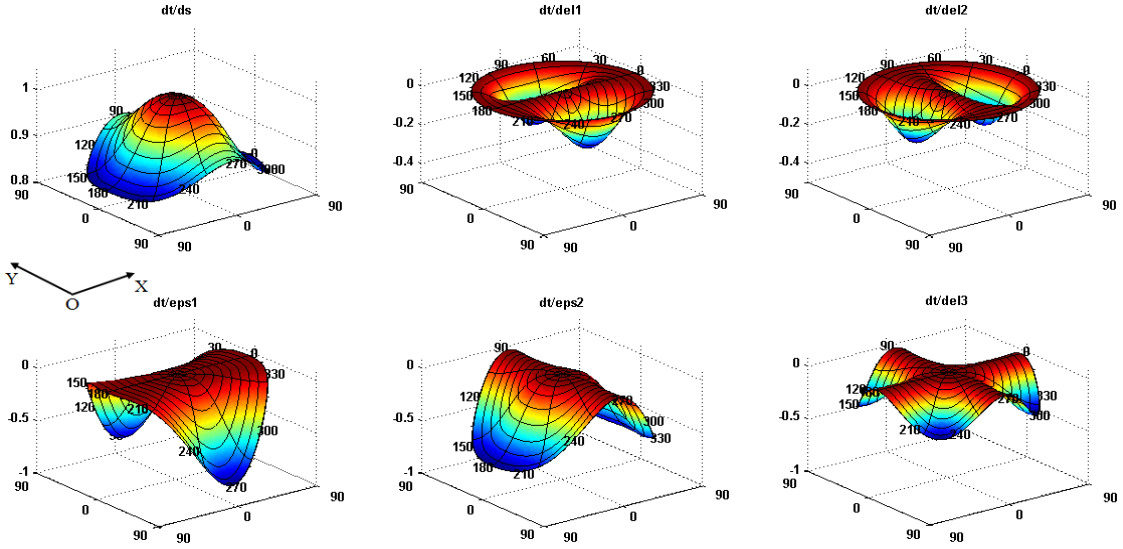

Figure 2 *The derivatives of orthorhombic parameters for $\varepsilon^{(1)}$=0.1, $\varepsilon^{(2)}$=0.2, $\delta^{(1)}$=0.06, $\delta^{(2)}$=0.12, $\delta^{(3)}$=0.05. Vertical axis represents the value of the derivatives. Azimuths are plotted from 0 to 360° with an interval of 30°.Polar angles are plotted from 0 to 90°.*

With these derivatives, the orthorhombic tomography can be built as a linear equation system to minimize the residual moveout of gathers for all azimuths. Checkshots' travel times can be used by ray tracing in orthorhombic media as additional constraints to minimize the mistie.

Application

We demonstrate the ability of our method to perform multi-azimuth imaging in the presence of orthorhombic anisotropy by building ORT models for OWAZ data sets. The Kepler and Justice

orthogonal WAZ surveys were acquired offshore Louisiana in the Mississippi Canyon of the GoM (Figure 3). For the study area, one large overhanging salt body dominates the survey. The rising up of the salt caused faults in surrounding sediment layers (Figure 4).

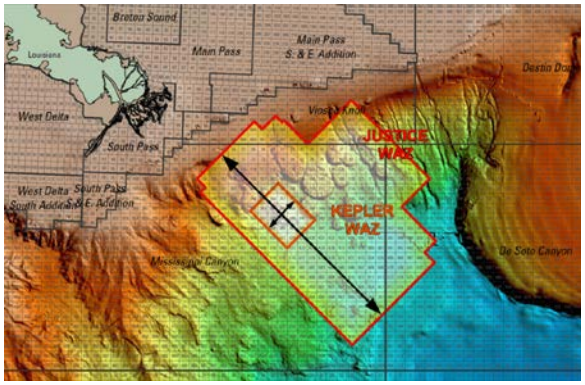

Figure 3 *Map showing the orthogonal surveys.*

A hybrid algorithm that combines fault detection with dip detection was used to produce the display in the study area (Figure 4). The slice (upper) is at a depth of 6,850 meters. The seismic cross-section (lower) shows a well-defined anticline that borders the salt dome approximately in the middle of the slice. The slice also shows a trend for the anticline that goes from the upper left toward the lower right. From the slice it can be conjectured that the salt dome, which has a left to right orientation, rose through the surrounding sediments. The faulting, which is well defined along the top of the anticline, follows the trend of the anticline itself. The faulting may be created by the buckling of the anticline with possible fractures aligned parallel to the faults themselves. The complex geology caused uneven stress and azimuthal anisotropy.

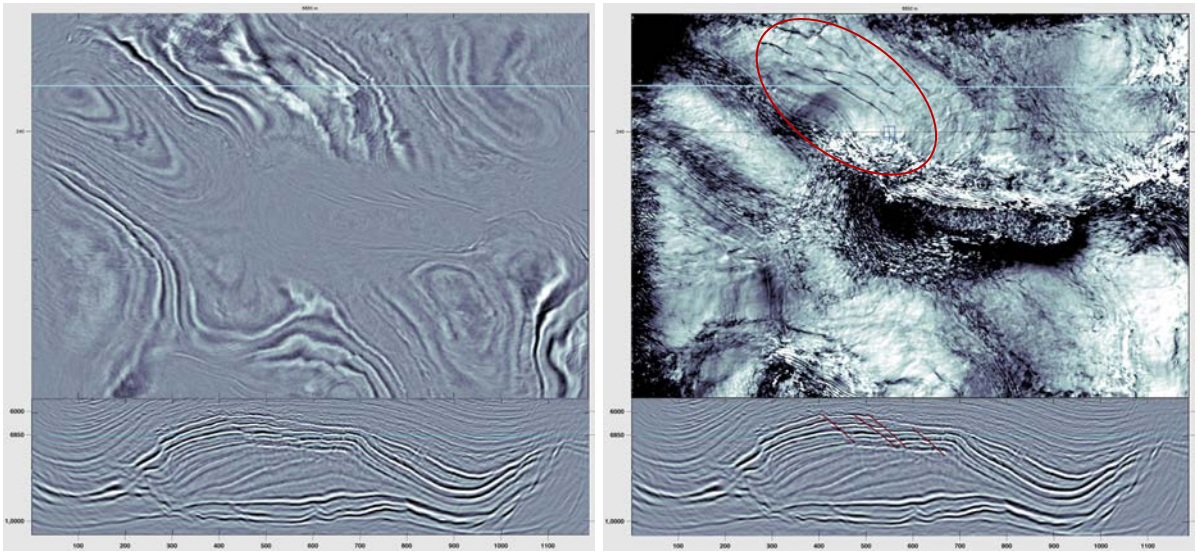

Figure 4 *On the top left is the horizontal slice of the seismic image in the study area, with a large salt body in the middle. On the top right is the coherence figure showing fault orientation. Faults are parallel to the trend of the anticline and go perpendicular to the salt boundary.*

In the final stage of TTI model building using OWAZ data,v_0, ε_0, δ_0, θ, and φ are used for an initial model for ORT imaging. The moveout discrepancy on CIGs from different azimuths is observed in some places (Figure 6A) due to the inability of simple TTI models to be realistic enough. The presence of orthorhombic anisotropy poses challenges in OWAZ imaging. With orthorhombic model building and migration, the image focusing is improved in the deep section, and the reflector underneath the carbonate zone has less fluctuation. This indicates simpler geologic structures (Figure 5) with the overburden models solving the conflicting moveout among azimuths (Figure 6B).

Conclusions

We introduced the process of orthorhombic model building and investigated the derivatives for orthorhombic tomography. By using our orthorhombic PSDM approach, we managed to account for anisotropy in both azimuthal and polar direction for the Kepler and Justice orthogonal WAZ data. Orthorhombic anisotropic PSDM reduced the structural discrepancies between seismic images built

for different azimuths, produced a constructive summation of OWAZ datasets and provided significant imaging uplift.

Acknowledgements

Authors would like to thank Zhiming Li, Laurie Geiger and Chuck Mason for reviewing the paper. We thank TGS management for permission to publish this paper.

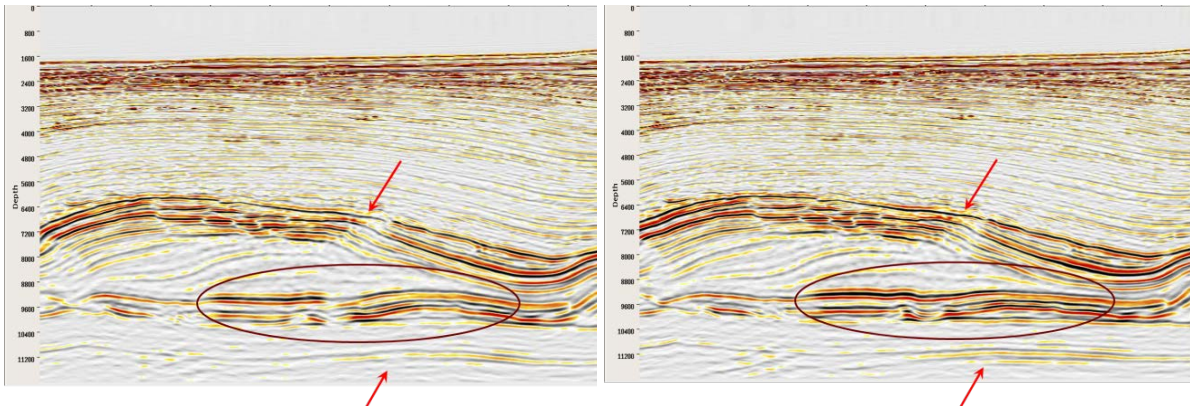

Figure 5 *The stacking images for the study area. On the left is the stacking image from the TTI final migration. On the right is the one from the orthorhombic migration.*

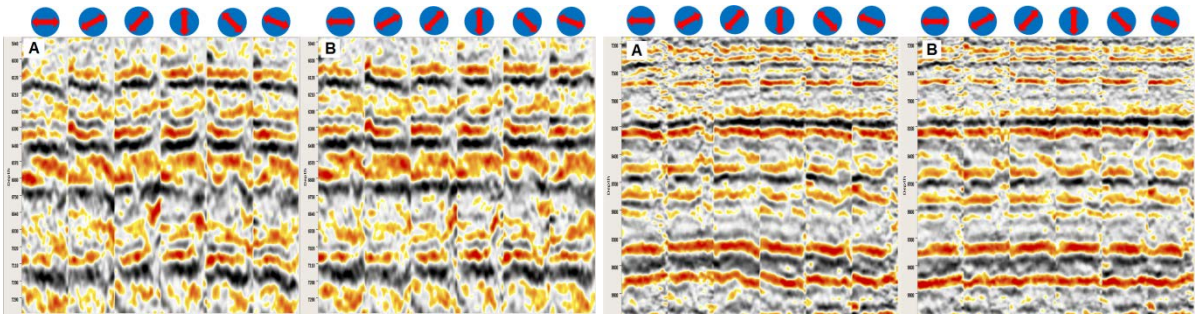

Figure 6 *Comparison of two different CIG locations for six azimuths extracted from the study area. A) The gathers from the final TTI migration. Inconsistency of the residual moveout is observed through different azimuths. B) The gathers from the orthorhombic migration. Gather flatness is improved among all azimuths. Azimuths are from 0 to 150˚ with an interval of 30˚.*

References

Baldock, S., C. Reta-Tang, B. Beck, W. Gao, E. Doue and S. Hightower, 2011, Orthogonal wide azimuth surveys: Acquisition and Imaging, SEG Expanded Abstracts, 147-151.

Gersztenkorn, A. and Marfurt, K., 1999, Eigenstructure based coherence computations as an aid to 3-D structural and stratigraphic mapping. Geophysics, 64(5), 1468–1479.

Howard, M., 2007, Marine seismic surveys with enhanced azimuth coverage: Lessons in survey design and acquisition. The Leading Edge 26, 480.

Li, Y., Han, W., Chen, C., and Huang, T., 2012, Velocity model building for tilted orthorhombic depth imaging. SEG Expanded Abstracts: 1-5.

Moldoveanu N. and Kapoor, J., 2009, What is the next step after WAZ for exploration in the Gulf of Mexico? 79th Annual International Meeting, SEG, Expanded Abstracts 28, 41.

Thomsen, L., 1986, Weak Elastic Anisotropy, Geophysics, 51, 1954-1996.

Tsvankin, I., 1997, Anisotropic parameters and P-wave velocity for orthorhombic media: Geophysics, 62, 1292-1309.